# The Crystal Ball Gazing with Electrostatic Precipitators: V-I Curves Analysis

V. Arrondel[1], G. Bacchiega[2], M. Hamlil[1], N. Gautier[3], A. Renard[3]
(1 EDF R&D – 6, quai Watier – 78 401 Chatou - FRANCE E-mail: veronique.arrondel@edf.fr
2 IRS srl - via Vigonovese 81 - 35124 Padova - ITALY E-mail: bacchiega@irsweb.it
3 EDF- Site de production de Cordemais, 44360 CORDEMAIS – France E-mail: alain.renard@edf.fr)

**Abstract:** Have you dreamed about knowing what happens inside an electrostatic precipitator (ESP) without opening it? Well, the main defects can be revealed using voltage - current curves. When the unit is operating, it is impossible to intervene in the electrofilter. Many parameters can be used to demonstrate an increase in dust emission levels which might result in a malfunctioning of the ESP itself or of other components of the unit. When the external elements of the electrostatic precipitator have been eliminated, attention can be focused on the Electrostatic precipitator itself. If a diagnosis can be performed “in state” before shutting down the unit, valuable gains can be made in time and efficiency during the maintenance operation. V-I curves constitute an invaluable aid, indeed, they are the signature of the ESP itself and are more precise than the maximum recorded voltage and current points. The voltage-current curves were obtained in experimental pilot conditions and in an industrial situation to demonstrate the four main defects most commonly encountered in ESP:

- the fouling of the emissive wires;
- the misalignment of plates and wires;
- insulators problems;
- the presence of back-corona.

In parallel, a modelling of the physical phenomena corresponding to these defects confirmed the modification of the curve. So, it is possible to predict the defects by analysing the V-I curves. To facilitate the V-I curves analysis of a significant size ESP, software was created in order to give:

- a display by field and file, the V-I curves;
- a comparison of different sets of data to follow the evolution of the curves;
- a defect mapping (clogging, misalignment or insulators problem, back-corona).

Subsequent validation on different ESP of the EDF fleet confirmed the power and the reliability of the software.

**Keywords:** V-I curves, software, EDF

## 1 ESP OPERATION AND MAINTENANCE

In coal-fired power plants, electrostatic precipitators (ESP) are the most widely used industrial system for collecting fly ash produced by combustion.

The operation and maintenance of an electrostatic precipitator may prove to be difficult because of the great number of physical processes involved: an electrostatic filter is at the same time a mechanical machine (rapping system, structure of the emitting wire and collecting plates), an electrical machine (high voltage power supply, electrical discharge), a fluid-dynamic machine (flow distribution and regulation) and a “chemical machine” (ash characteristics and flue gas conditioning).

When the emission level at the ESP outlet is too high, it must be remembered that there are many factors in play, distinct from the ESP itself. In fact, it starts upstream in the coal stockyard and finishes downstream in the chimney.

If the initial checks indicate that the electrostatic precipitator is in question, a reading of the voltage-current curves may allow a pre-diagnosis to be carried out.

The common operating problems are:

(1) Excessive Fouling of Discharge Electrodes;

(2) Excessive fouling of Collecting Electrodes;

(3) Reduced spacing between wires and plates (misalignment, bent electrodes, swinging electrodes);

(4) Broken electrodes;

(5) Dust building up in hoppers;

(6) Cracked wires support insulator.

On large ESP, the duration of the shut-down of the unit may be reduced if the origin of the defect can be identified beforehand. How can this be achieved on an electrofilter powered by 32 TR sets, composed of 2 boxes, each including 5 fields? These same fields are composed of 100 channels. It is like looking for a needle in a haystack!

Moreover on the rare occasion when the unit is shut down for the weekend, there is not enough time to carry out a complete inspection of the electrostatic precipitator.

This pre-diagnosis is carried out using the only parameters available under operating conditions: the voltage-current curves, which are the signature particular to each electrostatic precipitator.

## 2 VOLTAGE AND CURRENT: THE KEY PARAMETERS

The electric parameters represent a key factor in the performance of electrostatic precipitators.

The systems used to regulate electric power supplies vary greatly. However, they all operate using the same basic principle: the power supply system is designed to provide voltage to the electrical field (or bus section) at the highest possible level. However, the voltage must be controlled in order to avoid arcing or sparking between the electrodes and the plates, moreover it prevents back-corona.

In the absence of back-corona, the ideal automatic voltage control would produce the maximum collecting efficiency by holding the operating voltage of the precipitator at a level just below the spark-over voltage. But this level cannot be predicted from one instant to the next. Instead, the automatic voltage control increases output from the transformer-rectifier until a spark occurs. Then the control resets to a lower power level, and the power increases again until the next spark occurs.

It is not possible to operate an ESP without some particles deposits being present on the electrodes. These deposits can lead to:

(1) Disruption of corona, affecting particle charging;

(2) Reduction of flashover voltage, affecting particle charging and collection;

(3) Particles returning to the flue gas during rapping.

Particle resistivity is a significant factor in determining ESP efficiency.

For highly resistive dusts, the electrical breakdown strength of deposited dust layers can be insufficient to support the voltage which is developed in the layers by the passage of the normal ESP operating current. When this happens, the effects are nearly all detrimental and include neutralization of the charge on particles in the flue gas and re-entrainment of previously collected particles and a reduction of the average ESP operating voltage.

## 3 V-I CURVES

### 3.1 Shape of V-I Curves

The voltage-current characteristics are mainly due to the geometry of the electrostatic precipitator, to the flue gas which passes between the plates (particle concentration, temperature, etc.) and to the electrical faults (misalignment, insulator fault). The position and form of the characteristic curve changes if a fault occurs.

In the absence of dust and under the same temperature, humidity and pressure conditions, and clean, identical fields have the same characteristic voltage-current curve (Fig .1).

Under normal operating conditions of the unit, the voltage-current curves are shifted because of:

(1) Changes in temperature, humidity and pressure of the flue gas

(2) Changes in particle density of the flue gas

(3) Particle layer resistivity at the electrodes

(4) Mechanical and electrical faults

Changing flue gas conditions modifies the electric discharge behaviour and consequently the V-I curves are shifted. Higher flue gas temperatures shift VI curves to the right as the electric discharge produces less current for the same applied voltage. An example of VI curve shift is given in Fig. 2, where the no load curve has a flue gas temperature of 40 ℃, while in the 4th field, almost no load curve, has a flue gas temperature of 140 ℃.

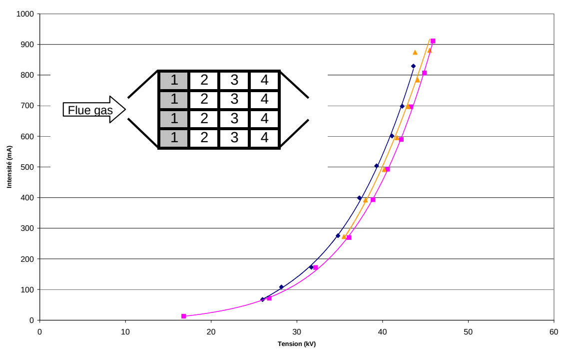


**Fig. 1** V-I curves of the 1st fields

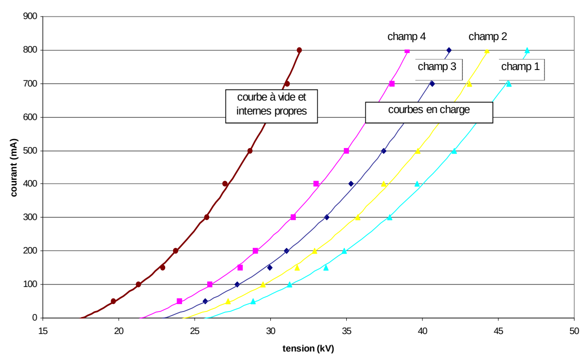


**Fig. 2** Simulation of the V-I curves for different fields (on-load and no load)

Changing particle density of the flue gas modifies the amount of charged particles and gives rise to the known effect as space charge. Particle charging has a screening effect, it lowers the electrical field in the wires and accordingly the current created by the electrical discharge. The current is therefore lower for the same voltage level. As shown in Fig. 2 in the first field, where the flue gas enters, the curve is located at the extreme right because of the higher particle density. In successive fields, as the particles are progressively collected, the particle density declines and the curves move to the left.

After a certain number of hours of operation, the electrostatic precipitator could have the following mechanical or electrical faults:

(1) Fouling of the plates or wires;

(2) Misalignment of wire/plate;

(3) Leakage from insulators.

These faults change voltage current curves. In order to observe, verify and quantify the effect of the faults on the ESP, it is possible to use two different methods: the experimental procedure or a simulation tool.

### 3.2 Fouling Effect on V-I Curves by the Experimental Procedure

To verify the fouling impact of the plates and the wires some experiments were undertaken on an industrial electrostatic precipitator.

#### 3.2.1 ESP description

The Cordemais power station has two identical units (units 4 and 5), that burn imported coal, with a rated output of 600 MWe. They are equipped with flue gas desulphurisation installation downstream from the electrostatic precipitator. The emission level must remain below 50 mg/Nm$^3$ (on dry flue gas with 6% $O_2$) to enable the desulphurisation unit to operate correctly. The electrostatic precipitator consists of two identical casings. Each casing contains 4 fields, with a plate-to-plate distance of 300 mm: four independent transformer-rectifier sets supply each field.

Between 14th and 18th April 2003, the unit 5 and electrostatic precipitator operating parameters were recorded, these included the complete coal analysis, unit load, oxygen rate at the stack and at the economiser, the ESP inlet temperature and the voltage for each TR set.

The unit was operating at stable power (510 MW). The coal burnt was a mixture of 3 coals: AFS/POL/USA, the composition of which is as follows:

(1) Sulphur content: 1.13%;

(2) Ash content: 14.15%;

(3) Volatile matter content: 30.28%;

(4) GCV: 7261 kcal/kg.

The current-voltage curves of the electrostatic precipitator were recorded using oscilloscope measurements. The analysis of the curves was followed by internal inspection of the filter casing, in order to identify the origin of any curve modification.

#### 3.2.2 Stop Rapping

In order to clean the elements inside the electrostatic precipitator, systems are used to rap the plates and the wires. These systems were taken out service separately to observe any changes to the current-voltage curves.

**Effect of Wire Fouling on V-I Curves (see Fig. 3)**

Without back-corona, we observe changes to the V-I curves of the second field under different conditions:

(1) With wires cleaned by continuous rapping with no load for 30 minutes;

(2) Normal rapping conditions;

(3) After a pause of 2 ½ hours in wire rapping,

(4) After a pause of one night (approximately 15 hours) in wire rapping.

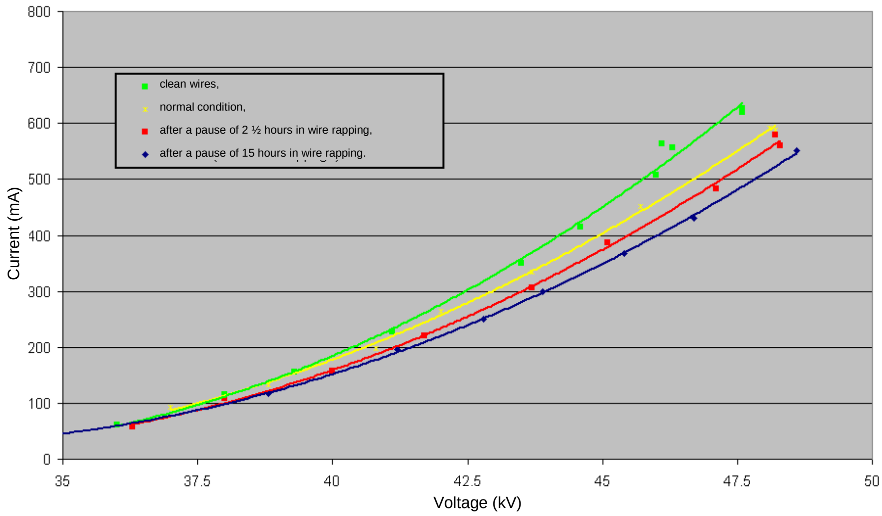


**Fig. 3** V-I curves evolution: clean wires, normal condition, after a pause of 2 ½ hours in wire rapping, after a pause of 15 hours in wire rapping

We observe that the fouling of the emitter electrodes leads to a shift to the right of the current-voltage curves. This shift may be explained in two ways:

(1) By a reduction of the corona effect due to an increase in the diameter of the emitter electrode due to fouling;

(2) By the electrical field reduction caused by a drop in voltage in the dust layer fouling the wire, resulting in a current decrease.

Fouling of wires reduces the level of the current at the same imposed voltage.

**Effect of Plate Fouling on V-I Curves (see Fig. 4)**

Without back-corona, we observe the V-I curves of the second field under different conditions:

(1) With plates cleaned by continuous rapping with no load for 30 minutes;

(2) Normal rapping conditions;

(3) after a pause of 2 ½ hours in plate rapping;

(4) after a pause of one night (approximately 15 hours) in plate rapping.

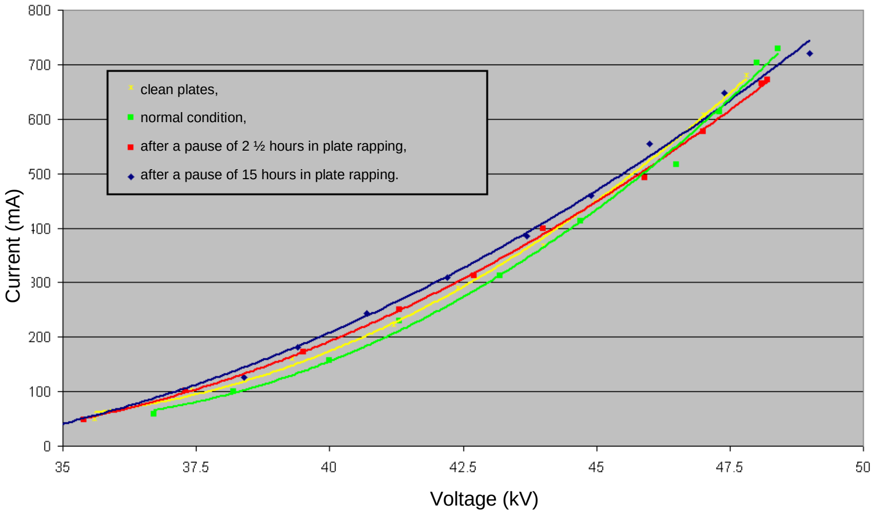


**Fig. 4** V-I curves evolution : clean plates, normal condition, after a pause of 2 ½ hours in plate rapping, after a pause of one night (approximately 15 hours) in plate rapping

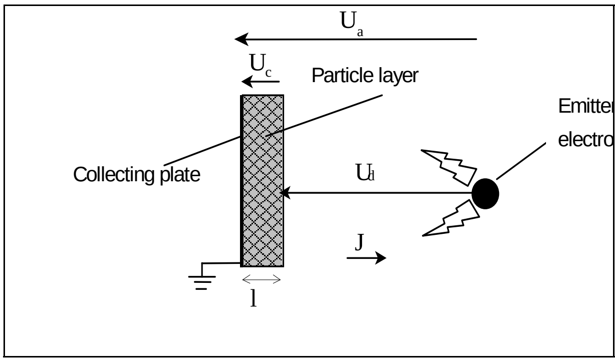


*J* the density of the current.

$U_d$ the difference in potential between the wire and the surface of the layer of dust. This is therefore the voltage available for the corona discharge on the emitter electrode.

$U_c$ the drop in potential through the layer of dust.

$U_a$ the voltage supplied by the transformer:

$U_a = U_d + U_c$

$l_c$ the thickness of the layer of dust $U_a$.

**Fig. 5** Typical electrostatic precipitator configuration

In the absence of back-corona, the V-I curves do not change when rapping is stopped; this confirms the observations made on the industrial pilot plant at Marghera power station [16].

However if the layer is resistive, a drop in voltage Uc occurs (Fig. 6), depending on the thickness of the layer and its resistivity.

With this modelling, the characteristic voltage current curve shifts to the right: fouling of the plates reduces of the level of current at the same imposed voltage.

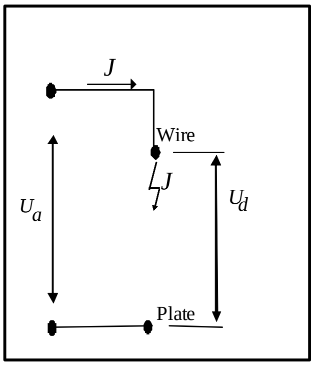


**Fig. 6** Equivalent electrical diagram of an electrostatic precipitator operating in normal conditions

### 3.3 Modelling Faults: Insulator Leakage and Back-corona

The deformation of voltage-current curves due to the presence insulator leakage and back-corona is illustrated below. The physical phenomena in question are described.

#### 3.3.1 Normal Operation

By applying a voltage $U_a$ between the electrode and the plate, the density of the current *J* supplied by the TR-set crosses the space between the electrodes.

In the absence of faults and back-corona and for a non-existent layer, the current voltage curve is approximated by the following equation:

$$J = k\left(aU_d^{\ 2} + bU_d + c\right) \qquad (1)$$

where: *a*, *b*, *c*, *d* are coefficients;

*k*, a constant which depends on the velocity of the gas;

*J*, the density of the current (measured in $10^{-5}$ A/m$^2$) on a plate at the voltage $U_d$ (measured in kilovolt) and the velocity of the gas *v* (measured in m/s).

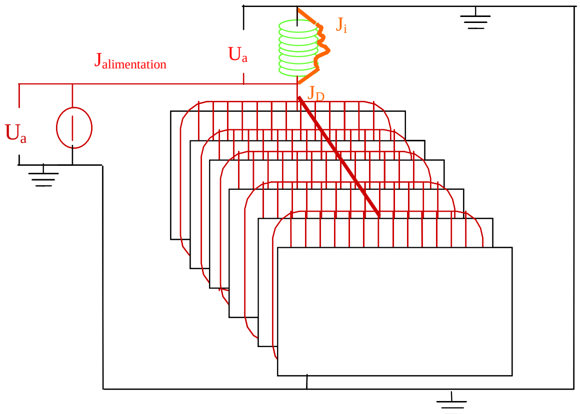


**Fig. 7** Equivalent electrical diagram with an insulator leakage

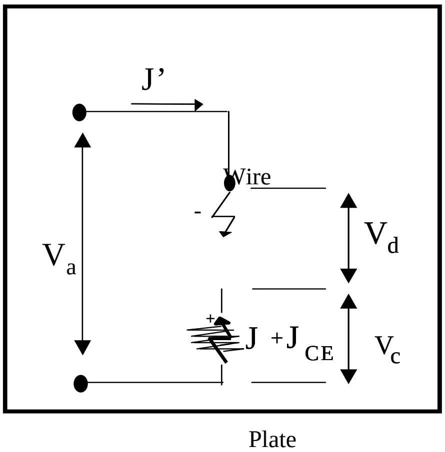


**Fig. 8** Equivalent electrical diagram of an electrofilter including the layer voltage drop and the back-corona current

### 3.3.2 Insulator Leakage

The insulators, which provide physical support for the electrodes supplied by the high voltage supply, may have operating faults: most commonly current leakage occurs towards the insulator to the detriment of the corona discharge (Fig. 7).

With this modelling, the characteristic voltage current curve shifts to the left: an insulator leakage produces an increase in the level of current at the same imposed voltage.

In the event of an insulator leakage, the voltage level supplied by the TR-set gradually drops off depending on the severity of the fault.

### 3.3.3 Back-corona

Modelling voltage current characteristics in an electrostatic precipitator with back-corona requires a representation of the particle layer. The particle layer is characterized by its electrical resistivity. In our model, the back-corona current adds to the current produced by the negative glow-corona discharge and so participates in the voltage drop in the particle layer.

The increased voltage drop creates a higher electric field that increases the back-corona current density and so in turn modifies the voltage drop. We have a positive feedback effect that is a typical phenomenon observed in the presence of

To quantify the electrical current passing through the insulator, a quadratic law links the density of the current $J_i$ to the voltage applied across the terminals of the corresponding insulator at the supply voltage $U_a$.

$$J_i = kU_a^2$$

where: $J_i$ is the density of the current expressed in mA/m$^2$;
$U_a$ is the supply voltage expressed in kV;
$k$ is a coefficient expressed in mA/(kV)$^2$·m$^2$;
$k$ varies from $10^{-6}$ mA/V$^2$/m to 1 mA/V$^2$·m$^2$.

The estimation of the back-corona current density $J_b$ is based on the electric field in the particle layer $E_l$. A typical quadratic relationship has been assumed and corrected for the particle layer thickness l:

$$J_b = k_b l^{0.4} \left( E_l - E_t \right)^2 \qquad (2)$$

kb is a constant.

$$\begin{cases} J' = J(U_d) + J_b \\ E_l = \rho\, J' \\ U_a = U_d + E_l l \end{cases} \qquad (3)$$

back-corona.

It is possible to identify the voltage-current electrostatic precipitator working point including the positive feedback using the following equations:

The computed influence of particle layer resistivity on the voltage-current characteristics are shown in Fig. 9. The characteristics for low dust resistivity are virtually identical with that obtained with a clean plate. As the resistivity value increases the current value increases as well. The current rise can be so high that it limits the achievable applied voltage.

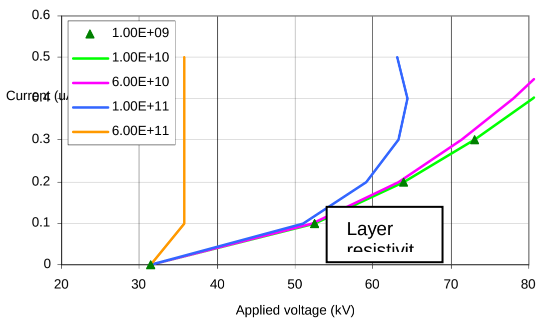


**Fig. 9** Voltage-current characteristics as functions of layer resistivity

The back-corona current varies also as function of particle layer thickness and flue gas characteristics.

### 3.3.4 V-I curve Interpretation

The V/I curves are the "signature" of an electrostatic precipitator. They may be plotted field by field, on-load and no load. The plotting and the analysis of on-load curves are very useful for identify faults. There are at least 3 "abnormal" cases, the causes of which may be readily pinpointed thus limiting the additional investigations required.

**case 1**: a much "steeper" rise in current than the reference indicates that back-corona has developed.

**case 2**: shifts in the position of the curves in relation to their normal positions:

- if the on-load curve of a field "moves" to the right of the normal curve, it is probably due to the fouling of the wires (Fig. 10),
- if the on-load curve "shifts" to the left of the normal curve: there is probably an insulator leakage or a mechanical failure inside this field, for example, a displaced electrode. Repairs require the shutting-down of the unit.

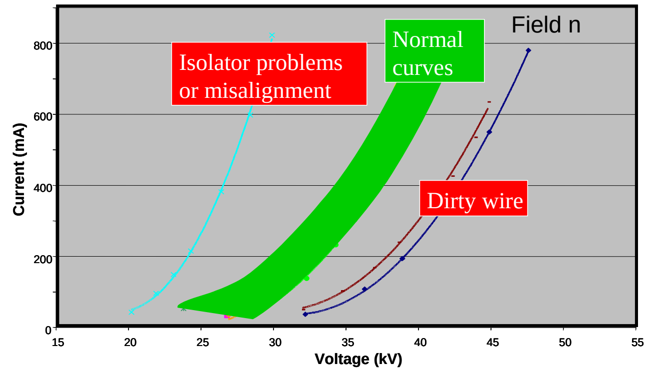


**Fig. 10** Fault identification by the superposition of V-I curves of several fields

**case 3**: Normal curve but spark point lower than on the reference curve, the most common cause is a broken wire.

## 4 A TOOL FOR EASY INTERPRETATION OF V-I CURVES

### 4.1 Functionalities of the software

A computer tool has been developed to facilitate the analysis of the current-voltage curves of electric precipitators equipped with more than 10 electrical power supplies and to compare these curves plotted at different loads or during the combustion of different coals.

The tool allows for the creation of a reference curve for each field. The reference curve can be computed by averaging VI curves under different flue gas and combustion conditions. Depending on boiler combustion and flue gas conditions, different reference curves could be needed.

The tool then automatically identifies the following faults: wires fouling, reduced spacing between wires and plates, insulator leakage. The tool is able to recognize also back-corona presence and faults under back-corona conditions.

Faults can be identified by comparing the curve of the bus section concerned with a reference one and by calculating the average distance between these two curves.

It then automatically generates an analysis report for a convenient overview of the faulty fields.

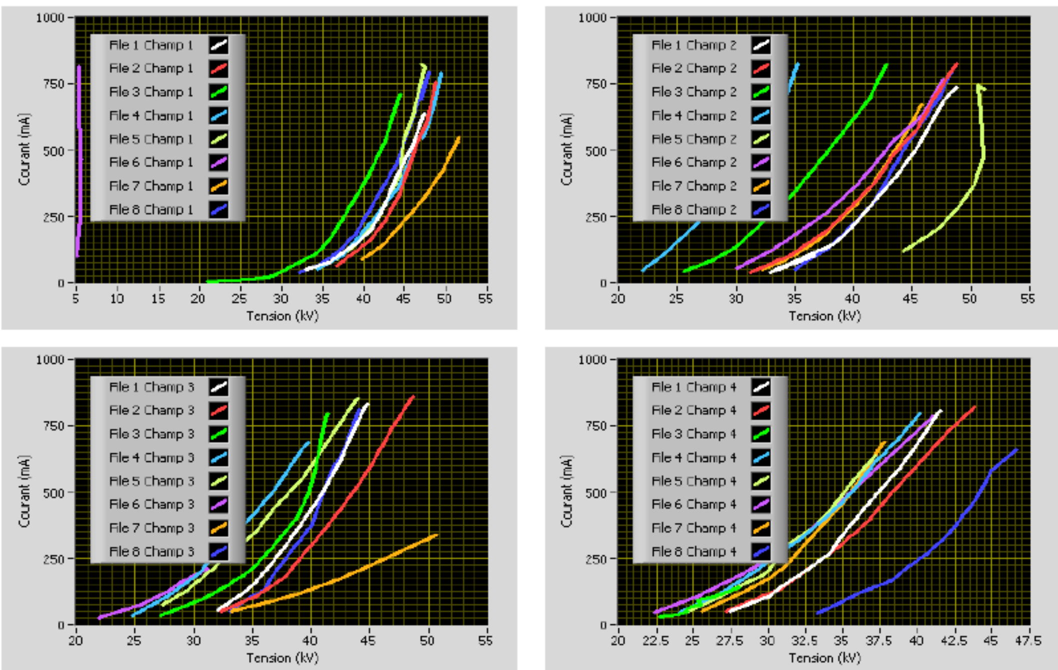

Casing 2

| | Field.1 | Field.2 | Field.3 | Field.4 |
|---|---|---|---|---|
| File. 5 | 211 | 221 CE-ENC | 231 | 241 |
| File. 6 | 212 CC | 222 | 232 | 242 |
| File. 7 | 213 ENC | 223 | 233 ENC | 243 |
| File. 8 | 214 | 224 | 234 | 244 ENC |

**Legend**

| | |
|---|---|
| OK | (green) |
| Fault | (red) |
| Insufficient data | (grey) |

**Fault type**

| | |
|---|---|
| Misaligment - insulator leakage | DA/FI |
| Important fouling | ENC |
| Back-Corona | CE |
| Short-circuit | CC |

**Fig. 11** Reports of the tool

### 4.2 Validation

#### 4.2.1 Description of the Tests

The tool has been validated during tests carried out on unit 5 of Cordemais. This was done in two steps.

The first consisted in plotting current voltage curves under stable unit operating conditions: the **readings** were made using an **oscilloscope.**

The second stage was a detailed inspection of the visible faults inside the electrostatic precipitator. This inspection focussed on one casing of the ESP.

For each bus section, it enabled us to compare the faults detected by the tool and those found during the inspection.

The photos illustrating the faults identified during the visit are given in the table below:

ESP 2

| | Field.1 | Field.2 | Field.3 | Field.4 |
|---|---|---|---|---|
| File. 5 | 211 clean wires no photo | 221 view from field entry fouling wires 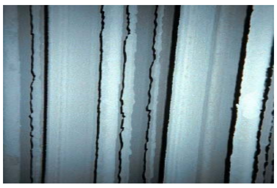 | 231 clean wires  | 241 clean wires 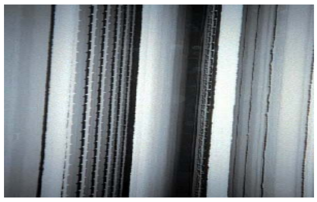 |
| F. 6 | 212 clean wires no photo | 222 clean wires 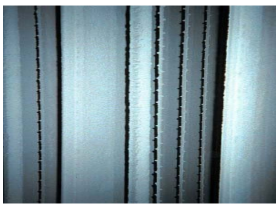 | 232 clean wires 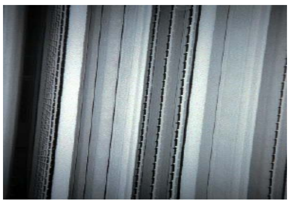 | 242 clean wires 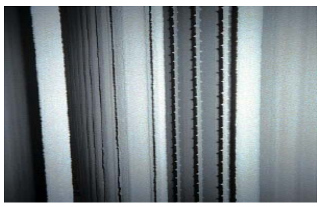 |
| F. 7 | 213 upper part fouling wires | 223 clean wires | 233 view from field entry fouling wires | 243 clean wires |


F. 8

#### 4.2.2 Comments

The summary of the faults analysis by the V-I tool is given in Fig. 11.

For casing 2 of Cordemais 5, the state of the quarter fields detected by the V-I tool and that found during the inspection, are as follows:

| Field | Visit inside the ESP | Default detected by U-I tool | Remark |
|---|---|---|---|
| 211 | NR | NR | OK |
| 212 | Misalignment | Short-circuit | (1) |
| 213 | Fouling | Fouling | OK |
| 214 | NR | NR | OK |
| 221 | Fouling | Back-corona - Fouling | (2) |
| 222 | NR | NR | OK |
| 223 | NR | NR | OK |
| 224 | NR | NR | OK |
| 231 | NR | NR | OK |
| 232 | NR | Insufficient data | OK |
| 233 | Fouling | Fouling | OK |
| 234 | NR | NR | OK |
| 241 | NR | NR | OK |
| 242 | NR | NR | OK |
| 243 | NR | NR | OK |
| 244 | Uncompleted visit | Fouling | (3) |

NR : Nothing to Report

(1) The tool detects a short-circuit since the supply voltage of this quarter field is very low, probably due to the considerable misalignment of the plates, as recorded during the inspection of the electrostatic precipitator.

(2) The detection of a single back-corona is not significant, indeed if a single quarter field detects back-corona, the measurement may be called into question.

(3) The incomplete inspection of the quarter field did not enable us to see the fouling which is probably located in the top part of the quarter field. This part is difficult to reach.

The tool detected faults of the “fouling of wires or plates”, short-circuit or back-corona type correctly. Misalignments were noted during the inspection of the electrostatic precipitator. These misalignments are not significant enough to be observable on the V-I curves, as shown by the simulations carried out using the ORCHIDEE [16] software.

## 5 CONCLUSIONS

The voltage-current characteristics are mainly due to the geometry of the electrostatic precipitator, the flue gas characteristics which pass between the plates (e.g.: concentration, temperature, etc.) and to electrical faults (e.g.: misalignment, insulator leakage). The position and form of the characteristic curve changes if a fault occurs. This curve may therefore be used to identify faults. These curves are the “signature” of an Electrostatic precipitator.

After measuring the current-voltage characteristics, it is important to compare the values measured. It is useful to define a reference curve computed by averaging same field V-I curves (excluding obvious faults) and if necessary using multiple measurements under the same operating conditions.

Comparing each curve with its reference permits the following interpretation to be made:

a) if the curve is “more to the right” (i.e. for a certain voltage level there is less current than on average), the possible fault is fouling of the wires (the rapping is not efficient),

b) if the curve is “more to the left” (i.e. for a certain voltage level there is more current than on average), the possible faults are:

- Problems with the insulators,
- Misalignment.

c) if the current voltage curve tends towards the vertical, there is back-corona.

The identification of faults by automatic analysis of V-I curves facilitates interventions for maintenance.

**REFERENCES**


1. J. SALVI. A methodology to simplify the ESP models. VIII ICESP*, Birmingham – USA, 2001.
2. I. GALLIMBERTI, The Simulation of Corona Discharges Under Practical Precipitator Conditions, Symposium on the Transfer and Utilisation of Particulate Control technology-EPRI-New Orleans, Vol. 1, November 1986
3. B. BELLAGAMBA, F. MATTACHINI, I. GALLIMBERTI, R. TURRI, A. GAZZANI, U. TROMBONI. A Mathema-tical Model for Simulation of Large Scale Electrostatic Precipitators. 5th International Conference on Electrostatic Precipitation, Washington D.C., 1993.
4. I. GALLIMBERTI, A. GAZZANI, U. TROMBONI, E. LAMI, F. MATTACHINI, G. TREBBI. Physical simulation of the particle migration in ESP, Part I - Model description. VI ICESP*, Budapest, 1996.
5. I. GALLIMBERTI, A. GAZZANI, U. TROMBONI, E. LAMI, F. MATTACHINI, G. TREBBI. Physical simulation of the particle migration in ESP, Part II - Application results. VI ICESP*, Budapest, 1996.
6. E. LAMI, F. MATTACHINI, I. GALLIMBERTI, R. TURRI, U. TROMBONI. A Numerical Procedure for Computing the Voltage-Current Characteristics in ESP Configuration. Journal of Electrostatics 34 (1995) 385-399, 1994.
7. I. GALLIMBERTI. Recent advancements in the physical modelling of electrostatic precipitators. Journal of Electrostatics 43 (1998) 219-247, 1998.
8. V. ARRONDEL, G. BACCHIEGA, I. GALLIMBERTI. ESP modelling: from University to Industrial Application. VIII ICESP, Birmingham – USA, 2001.
9. I. GALLIMBERTI. Detailed mass balance in electrostatic precipitators under industrial operating conditions. Invited Masuda Lecture, Opening plenary session, IX ICESP, Kruger – South-Africa, 2004.
10. G. BACCHIEGA, I. GALLIMBERTI, V. ARRONDEL, PH. RAIZER, J. LECOINTRE, M. HAMLIL. Static and dynamic back-corona characteristics. IX ICESP, Kruger – South-Africa, 2004.
11. V. ARRONDEL, J. SALVI, I. GALLIMBERTI, G. BACCHIEGA. ORCHIDEE: Efficiency Optimisation of Coal Ash Collection in Electrostatic Precipitators. IX ICESP, Kruger – South-Africa, 2004.
12. R. BICKELHAUPT. A technique for Predicting Fly Ash Resistivity. Rapport EPA-600/7-79-204. August 1979.
13. R. BICKELHAUPT. Fly Ash Resistivity Prediction Improvement With Emphasis on Sulphur Trioxide. Rapport EPA-600/7-86/010. March 1986.
14. G. BACCHIEGA, I. GALLIMBERTI, E. SANI, R. SALA, V. ARRONDEL, M. HAMLIL, E. CHRISTENSEN. Experimental study of the mass balance in a pilot industrial. J. of Electrostatics July 2005.
15. V. ARRONDEL, N. CARAMAN, M. HAMLIL, G. BACCHIEGA, I. GALLIMBERTI. Development of an industrial model of rapping - effect on the collecting efficiency. X ICESP, Cairns - Australia, 2006.
16. G. BACCHIEGA, I. GALLIMBERTI, V. ARRONDEL, N. CARAMAN, M. HAMLIL. Back-corona model for prediction of ESP efficiency and voltage-current characteristics. X ICESP, Cairns – Australia, 2006.
17. V. ARRONDEL, J. SALVI, I. GALLIMBERTI, G. BACCHIEGA. ORCHIDEE: Efficiency Optimisation of Coal Ash Collection in Electrostatic Precipitators. IX ICESP, Kruger – South Africa, 2004.